VALIDATION OF SATELLITE DERIVED PRIMARY PRODUCTION MODELS IN THE NORTHEAST ATLANTIC

P.V. Lobanova [(1)], I.L. Bashmachnikov [(1), (2)], V. Brotas [(3)]

[(1)] *Saint-Petersburg State University, Institute of Earth Science (Russia, St. Petersburg), Email: pl19@mail.ru*
[(2)] *NIERSC- Nansen International Environmental and Remote Sensing Centre (Russia, St. Petersburg), Email: igorb1969@mail.ru*
[(3)] *MARE – Marine and Environmental Sciences Centre, Faculdade de Ciências, Universidade de Lisboa (Portugal, Lisbon), Email: vbrotas@fc.ul.pt*

ABSTRACT

With all the variety of models used for calculation of primary production of phytoplankton (*PP*) from remote sensing data, a choice of the most realistic one for a particular ocean region remains a non-trivial issue. In this work, we estimate *PP* in the Northeast Atlantic Ocean (20^0 - 51^0 N and 10^0 – 40^0 W) from 1998 to 2005 using three frequently used models: VGPM (Vertically Generalized Production Model), PSM (Platt and Sathyendranath Model) and Aph-PP model (Absorption Based Model). The modeled results are then compared with *in situ* observations of *PP*. The results show a close similarity in *PP* patterns obtained by different models, but the absolute modeled values differ substantially. In the Northeast Atlantic, PSM is found reproducing better the observed seasonal and spatial variability of *PP* as compared to the two other models. However, PSM slightly underestimates the *PP* values.

1. INTRODUCTION

Phytoplankton transform dioxide carbon and water into organic matter through photosynthesis using sun energy. An amount of generated organic matter per unit time can be estimated by primary production of phytoplankton (*PP*). Daily *PP* integrated through euphotic zone can be obtained from direct *in situ* measurements or calculated from empirical (or semi-empirical) models. The latter estimate *PP* using relations between photosynthesis and available light [1]. Some main model parameters may be defined remotely by satellite observations that cover almost the whole World Ocean and permit estimation of different bio-optical parameters with high spatial and temporal resolution. In particular, various satellite derived models for estimation of *PP* are proposed [2 - 6]. However, its application provides different results, and a choice of the most realistic one is often a regional issue, which should take into account regional dependence of photosynthetic efficiency on hydro-optical and bio-chemical conditions. Therefore, to obtain good match ups with *in situ* observations of *PP*, satellite derived models should also take into account peculiarities of regional ecosystems.

In this work, we estimate *PP* in the Northeast Atlantic Ocean (20^0 - 51^0 N and 10^0 – 40^0 W) from 1998 to 2005, using three famous models: two models are based on a chlorophyll-a concentration (VGPM and PSM) and one – on an absorption coefficient of phytoplankton (Aph-PP). The model results are then compared with *in situ* observations in the study region. The models use as an input level 3 Ocean Colour data downloaded from the OC-CCI database version 1 (http://www.esa-oceancolour-cci.org). Photosynthetic model parameters were obtained from experimental measurements of photosynthetic efficiency under different light conditions for Northeast Atlantic phytoplankton communities.

2. METHODS AND DATA

2.1. Primary production models

Three primary production models are used in this study. Two of them are based on chlorophyll-a concentration: VGPM (Vertically Generalized Production Model) [4] and PSM (Platt and Sathyendranath Model) [7]. The basis of the third Aph-PP model (Absorption Based Model) [3] is an absorption coefficient of phytoplankton, which also can be defined from satellite derived ocean Colour data.

Maximum photosynthetic efficiency in **VGPM** [4] is described as optimal rate of photosynthesis (P^B_{opt}) in water column normalized to chlorophyll-a concentration [mg C (mg Chl)$^{-1}$ h^{-1}]. The authors of the model suggested to express P^B_{opt} as a function of sea surface temperature (SST) [4]. VGPM estimates daily integrated *PP* in water column of euphotic depth (PP_{eu}) [mg C m^{-2} day^{-1}] as:

$$PP_{eu} = Chla \times P^B_{opt} \times \left(0.66125 \times \frac{I_0}{I_0 + 4.1}\right) \times z_{eu} \times DL \quad (1)$$

Where *Chla* is chlorophyll-a concentration [mg Chl m^{-3}] (here and in the other two models used in this study, it corresponds to mean concentration in a layer of penetration depth “seen” by satellite spectroradiometers). I_0 is daily averaged surface photosynthetic active radiation at 400-700 nm (PAR) [E m^{-2} day^{-1}], z_{eu} is an euphotic depth [m] and *DL* is a day length [h].

The model uses the Baly curve [8, 9] to describe the light dependent photosynthetical function or photosynthesis - irradiance curve (*P-I* curve), which presents the dependence of photosynthesis on underwater illumination.

PSM (Platt and Sathyendranath Model) [7] estimates daily integrated *PP* at depth *z* (*PP(z)*) [mg C m^{-3} day^{-1}] using exponential photosynthetical function as:

$$PP(z) = Chla \times P^B_{max} \times \left[1 - exp\left(-\alpha^B \times \frac{I(z)}{P^B_{max}}\right)\right] \times exp\left(-\beta^B \times \frac{I(z)}{P^B_{max}}\right) \times DL \qquad (2)$$

Where P^B_{max} is maximum rate of photosynthesis [mg C (mg $Chl)^{-1}$ h^{-1}], α^B [mg C (mg $Chl)^{-1}$ h^{-1} (μE m^{-2} $s^{-1})^{-1}$] is the initial slope of the *P-I* curve and β^B is the photoinhibition parameter (same units as α^B). These three parameters are normalized to chlorophyll-a concentration. *I(z)* [μE m^{-2} s^{-1}] is irradiance at depth *z* and can be defined using exponential Beer–Lambert–Bouguer Law as a function of surface irradiance I_0:

$$I(z) = I_0 \times \exp(-k_d \times z) \qquad (3)$$

Here k_d is a diffuse attenuation coefficient of PAR [m^{-1}].

Aph-PP model [3] uses the absorption coefficient of phytoplankton (*aph*) [m^{-1}] as an input, at the wavelength 443 nm. This wavelength corresponds to a blue part of the light spectra. According to the authors of the model, usage of *aph* at 443 nm has one main advantage - minimization of an influence of Coloured dissolved organic matter (CDOM), which absorbs irradiance in the blue part of the spectra as chlorophyll-a does.

If photoinhibition is taken into account, daily integrated *PP(z)* [mg C m^{-3} day^{-1}] is calculated on a base of following relationship:

$$PP(z) = aph \times \left[\varphi_{max} \times \frac{K_\varphi}{K_\varphi + I(z)}\right] \times I(z) \times \exp(-\beta^B \times I(z)) \times DL \qquad (4)$$

Here the expression in square brackets is a quantum yield (or efficiency) of photosynthesis (φ) [mg C E^{-1}] – a ratio of photosynthetic rate (*P*) to *I*, presented by *φ-I* curve; φ_{max} is a maximum quantum efficiency at optimum light and K_φ [μE m^{-2} s^{-1}] is a half saturation constant [10]. *I(z)* is defined by Eq. 3.

PSM and APh-PP model estimate depth-dependent *PP(z)*, and for comparison with VGPM the Eqs. 2 and 3 are integrated from surface to euphotic depth. The euphotic depth is estimated using two methods. The first is Morel-Berthon algorithm [11] and the second is equation:

$$z_{eu} = \frac{\ln(100)}{k_d} = \frac{4.6}{k_d} \qquad (5)$$

Eq.5 follows from Eq.3, taking I_0 as 100% of incoming solar radiation.

The first method is used in VGPM algorithm (http://www.science.oregonstate.edu/ocean.productivity/vgpm.model.php), while for PSM and Aph-PP model the averaged euphotic depth of two methods above is used.

DL in all models is calculated using the astronomical algorithm as a function of a latitude and a day of a year (http://www.science.oregonstate.du/ocean.productivity/index.php).

2.2. Photosynthetic parameters

Photosynthetic model parameters of *P-I* and *φ-I* curves: α^B, P^B_{max} and φ_{max} are taken from experimental measurements of phytoplankton photosynthetic efficiency under different light conditions, for the phytoplankton communities of biological provinces of the Northeast Atlantic [6, 12-16]. The studies provide 29 values of P^B_{max}, 12 values of α^B and 13 values of φ_{max} for different seasons and locations. The final values of the photosynthetic parameters represent the averages of the values. In particular, the averaged φ_{max} value is very close to φ_{max}, obtained for cosmopolitan coastal phytoplankton diatom species - *Skeletonema costatum* in [18]. The *φ-I* curve for the species is used for deriving parameter $K\varphi$. The resulting value is less than suggested in [3]. Photoinhibition parameter β^B is taken from [17].

2.3. Satellite data

We used 8-days level 3 Ocean Colour data provided by the OC-CCI database version 1 (http://www.esa-oceancolour-cci.org). In the database chlorophyll-a concentration, the downwelling diffuse attenuation coefficient at 490 nm and the absorption coefficient of phytoplankton at 443 nm were obtained from the merged information of three radiospectrometers (SeaWiFS, MODIS, MERIS). The merged images has spatial resolution of 4×4 km. We filter 3 level Ocean Colour data assuming lognormal distribution of the parameters. A value is considered an outlier when its logarithm differs more than four standard deviations from the all-data-set time average for the corresponding point and date. To get stable statistics, instead of the one-point standard deviation we use its spatial average over the area of 80×80 km centered in the point.

As k_d in Eqs. 3 and 5 we use the downwelling diffuse attenuation coefficient at 490 nm.

8-days level 3 PAR were downloaded from the Ocean Productivity (NASA's OceanColor Web) database (http://www.science.oregonstate.edu/ocean.productivity/index.php). We use average values from two spectroradiometers SeaWiFS and MODIS. Preliminary analysis shows that difference between PAR values from two sensors is less than 3%. Therefore, using one sensor only instead of the average of the two, when another sensor is not available, does not input significant errors in the results.

SST data were downloaded from Multiscale Ultra-high Resolution Sea Surface Temperature database (http://mur.jpl.nasa.gov/InformationText.php), where the influence of clouds on the signal is particularly absent due to merge of infrared and microwave satellite temperatures from AVHRR, MODIS and AMSR. As daily SST data have 1x1 km spatial distribution, we average them into 4x4 km bins and over the 8-day time intervals, centered in the corresponding Ocean Colour dates.

2.4. *In situ* primary production data

In situ PP_{eu} data are obtained from [19-21]. Those measurements cover particularly all biological provinces of the Northeast Atlantic and were collected during different seasons in 1992 – 2005. The model derived PP_{eu} are averaged over the same areas and time intervals, as the presented observed values.

3. RESULTS AND DISCUSSION

Spatial distribution of daily PP_{eu} form three models described above has similar spatial and temporal patterns over the study area, but the values may differ substantially between the models. Fig.1 shows that the values increased in the areas of upwelling (Canary and Portuguese upwellings) and in the temperate area of the North Atlantic Current in the north. The minimum values are observed in the tropical part, south of the front of the Azores Current at around 35° N.

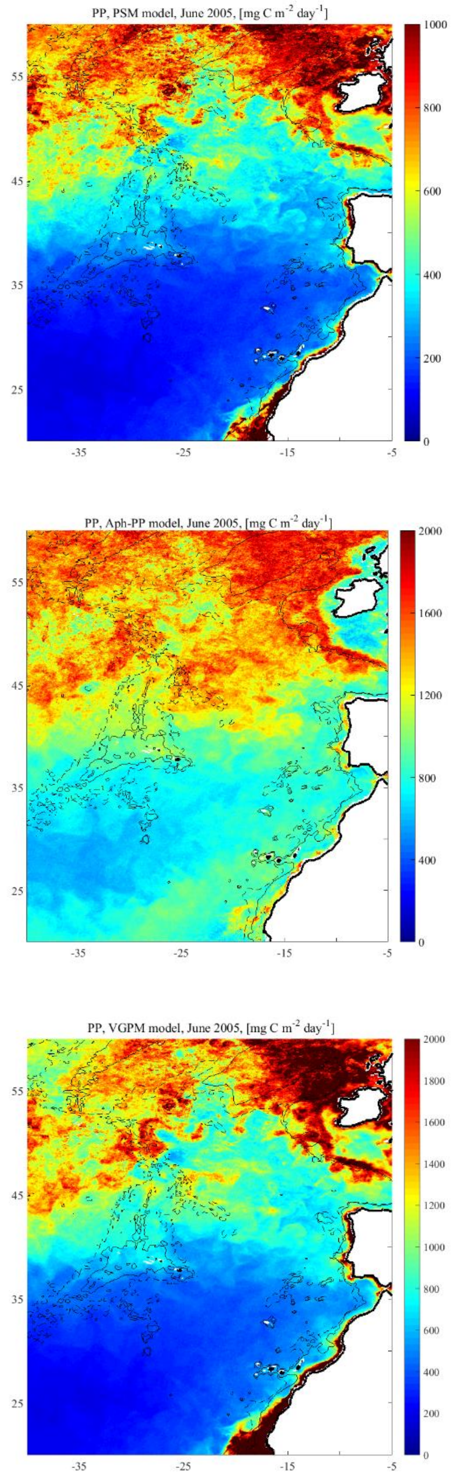

Figure 1. Monthly average PP_{eu} [mg C m^{-2} day^{-1}], obtained from VGPM, PSM and Aph-PP model for June 2005.

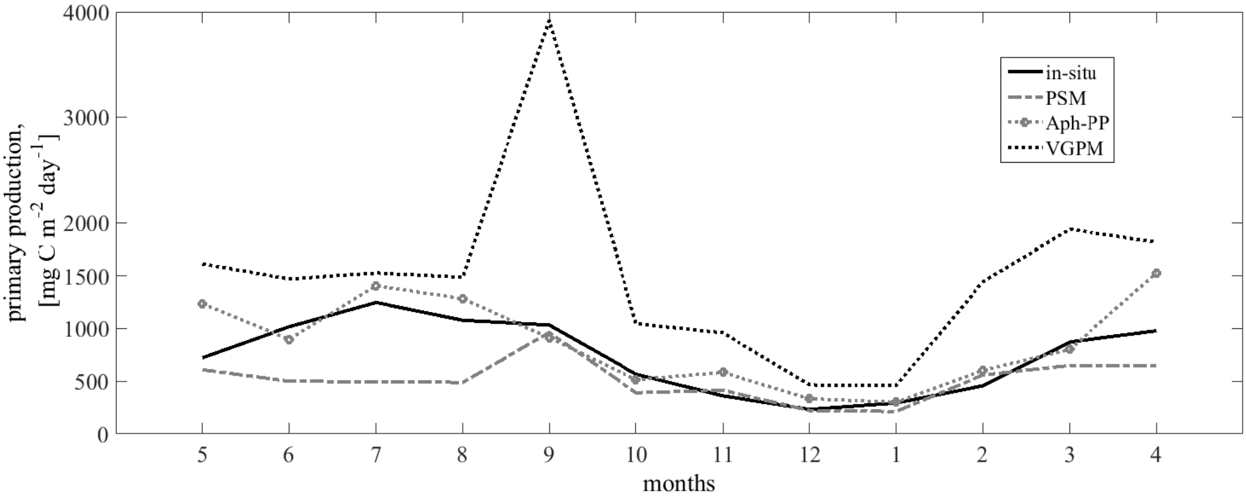

Figure 2. Comparison of monthly averaged modeled PP_{eu} [mg C m^{-2} day^{-1}] with in situ observations from May 2001 to April 2002 in the station at the Northwest shelf of Iberian Peninsula (42^0 07.8 N and 9^0 10.2 W) [21].

To validate the model results the derived PP_{eu} is compared with *in situ* observations in the Northeast Atlantic.

Fig. 2 shows observed and modelled seasonal variations of PP_{eu} from May 2001 to April 2002 at a station at the Northwest shelf of Iberian Peninsula (42^0 07.8 N and 9^0 10.2 W) [21]. The highest correlation of 0.8 (p-value<0.01) with *in situ* PP_{eu} is obtained for Aph-pp model. The correlation coefficients for PSM and VGPM are equal to 0.6 (p-value<0.05). PSM results also show a good match-up with *in situ* observations, especially during autumn-winter period, but underestimate PP_{eu} during spring and summer. VGPM overestimates PP_{eu}, and the difference with *in situ* data during some months (September 2001, March 2002) is more than twofold.

For further comparison, we use time and spatial averages of PP_{eu} for biological provinces, obtained from *in situ* measurements in [19 - 20]. In [20], the data were time and spatial averaged for each province during six expeditions in between 1998 and 2005 (May – June 1998, 2003, 2005; April – June 2004; September – October 2003, 2004, see Fig.3a).

In situ data from [19] were collected during five expeditions (April 1999, 2001; July – August 1998, October 2000, October – November 2001) in NAST(E) province (see caption to Fig. 3) and grouped by the authors into three zones (Fig. 3b). In this study, we use seasonally and spatially averaged data from each of the zone.

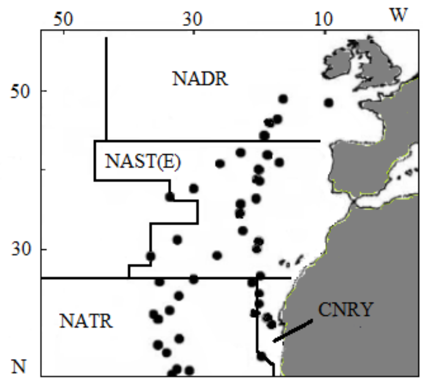

(a)

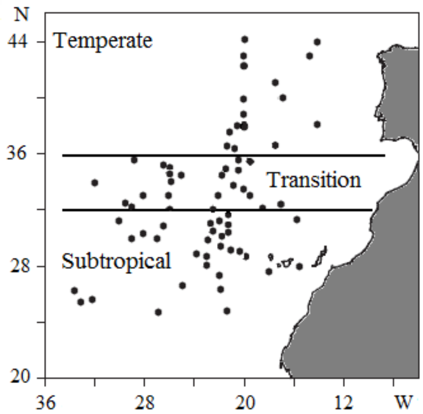

(b)

Figure 3. Positions of in situ PP_{eu} observations from [20] (a) and [19] (b). Biological provinces are: NADR – North Atlantic Drift, NAST(E) – North Atlantic Subtropical Gyre (East), NATR - North Atlantic Tropical Gyre, CNRY – Canary Current Coastal [22]. Temperate, Transition, Subtropical are determined in [19].

Table1. Relative difference (%) between modeled and *in situ* data of PP_{eu} in relation to *in situ* observations. Positive values mean that modeled PP_{eu} overestimates *in situ* observations, negative values – underestimates.

Region	VGPM			PSM			Aph-pp		
NADR[1]	107			-11*			128		
NAST(E)	74			-26*			190		
NATR	-23*			-64			135		
CNRY	156			-14*			66		
	Spring	Summer	Autumn	Spring	Summer	Autumn	Spring	Summer	Autumn
Temperate[2]	115	1660	50*	-9*	644	-34*	178	3024	93
Transition	95	231	111	-18*	50*	-8*	212	764	351
Subtropical	157	233	26*	4*	45*	-43*	339	725	223

*- difference less than 50% of *in situ* data

[1]Biological provinces according to [22]: NADR – North Atlantic Drift, NAST (E) – North Atlantic Subtropical Gyre (East), NATR - North Atlantic Tropical Gyre, CNRY – Canary Current Coastal (Fig.3a).

[2]Temperate, Transition, Subtropical are zones determined in [19] (Fig.3b).

The comparison of *in situ* and the model data are presented in Table 1.

PSM data has the best correspondence to *in situ* observations in the provinces NADR, CNRY and NAST(E) (-11, -14% and -26% respectively), while VGPM data are close to *in situ* in NADR (-23%).

PSM data also matches-up reasonably well *in situ* data in three zones of NAST(E) province, especially in spring and autumn. An exception is the Subtropical zone in autumn where VGPM shows the best fit (26%).

Aph-pp model significantly overestimates *in situ* observations in spite of a good correspondence at the station over the Iberian shelf (Fig.2), as well as in some other regions of the World Ocean [23, 24]. The reason of this difference has to be further investigated. It should be noted, that K_{φ} value we used in this study is less than suggested by the authors of Aph-pp model often used for estimating *PP* [23 - 25]. PP_{eu} calculated with K_{φ} value suggested by the authors is even higher.

VGPM model typically overestimates PP_{eu}. This was previously noted in [20] for NADR province. Overestimation may be due to errors in the optimal photosynthetic rate (P^B_{opt}), calculated as a function of SST [4]. However, this photosynthetic parameter also strongly depends on other factors, as nutrient supply, irradiance, dominating phytoplankton species, etc. Furthermore, satellite SST represents temperature only in the uppermost ocean layer, and P^B_{opt}, being a function of SST, differs in the lower layers, providing different photosynthetic efficiency.

In general, regional selection of the *P-I* curve parameters for the *PP* model permits improving the results.

4. CONCLUSION

Comparison of PP_{eu} obtained from the semi-empirical models with *in situ* observations in the Northeast Atlantic Ocean shows that the usage of regionally determined photosynthetic parameters taking into account regional dependence of photosynthetic efficiency of phytoplankton community on local hydro-optical and bio-chemical conditions, contributes to a better correspondence between the modelled and the observed *PP*.

PSM is found reproducing better the observed seasonal and spatial variability of PP_{eu} in the study region, as compared to the other two models. However, it slightly underestimates the PP_{eu} values.

5. ACKNOWLEDGEMENTS

The study was financially supported by grants of SPSU (St. Petersburg State University, St. Petersburg, Russia) № 18.55.1147.2014 and № 18.38.142.2014 and the grant of Russian Foundation for Basic Research (RFBR) № 16-05-00452.

The authors thank MARE – Marine and Environmental Sciences Centre of the University of Lisbon for the possibility to carry out the research and OC-CCI project and André B. Couto for helping with deriving satellite Ocean colour data.

6. REFERENCES

1. Zvalinsky, V.I. (2006). Process of primary production in the sea. *Izv. TINRO*, **147**, 276 – 302 (in Russian).
2. Eppley, R., Steward, E., Abbott, M. & Heyman, U. (1985). Estimating ocean primary production from

satellite chlorophyll: Introduction to regional differences and statistics for the Southern California Bight. *Journal of Plankton Research*, **7**, 57–70.
3. Lee, Z. P., Carder, K. L., Marra, J., Steward, R. G. & Perry, M. J. (1996). Estimating primary production at depth from remote sensing, *Applied Optics*, **35**, 463–474.
4. Behrenfeld, M. J., & Falkowski, P. G. (1997). Photosynthetic rates derived from satellite based chlorophyll concentration, *Limnology and Oceanography*, **42**(1), 1–20.
5. Behrenfeld, M. J., Boss, E., Siegel, D. & Shea D.M. (2005). Carbon-based ocean production and phytoplankton physiology from space, *Global Biogeochemical Cycles*, **19**, GB1006.
6. Smyth, T.J., Tilstone, G.H. & Groom, S.B. (2005). Integration of radiative transfer into satellite models of ocean primary production. *Journal of Geophysical Research, Oceans,* **110**(C10) article no. C10014.
7. Platt, T. & Sathyendranath, S. (1988). Oceanic primary production: Estimation by remote sensing at local and regional scales, *Science*, **241**, 1613–1620.
8. Baly, E. C. C. (1935). The kinetics of photosynthesis. *Proceedings of the Royal Society of London.* **117B**, 218-239.
9. Tamiya, H. (1951). Some theoretical notes on the kinetics of algal growth. *The Botanical Magazine, Tokyo*. **64**, 167-173.
10. Kiefer, D. A. & Mitchell, B. G. (1983). A simple, steady state description of phytoplankton growth based on absorption cross section and quantum efficiency, *Limnology and Oceanography*, **28**, 770–776.
11. Morel, A. & Berthon, J. F. (1989). Surface pigments, algal biomass profiles, and potential production of the euphotic layer: Relationships reinvestigated in view of remote-sensing applications, *Limnology and Oceanography*, **34**, 1545-1562.
12. Babin, M., Morel, A., Hervé, C., Bricaud, A., Kolber, Z. & Falkowski P.G. (1996). Nitrogen- and irradiance dependent variations of the maximum quantum yield of carbon fixation in eutrophic, mesotrophic and oligotrophic marine systems, *Deep Sea Research I*, **43**(8), 1241-1272.
13. Morel, A., Antoine, D., Babin, M. & Dandonneau, Y. (1996). Measured and modeled primary production in the northeast Atlantic (EUMELI JGOFS program): the impact of natural variations in photosynthetic parameters on model predictive skill, *Deep Sea Research I*, **43**(8), 1273-1304.
14. Kyewalyanga, M.N., Platt, T., Sathyendranath, S., Lutz, V.A. & Stuart, V. (1998). Seasonal variations in physiological parameters of phytoplankton across the North Atlantic, *Journal of Plankton Research*, **20**(l), 17-42.
15. Picart, S.S., Sathyendranath, S., Dowell, M., Moore, T. & Platt, T. (2013). Remote sensing of assimilation number for marine phytoplankton, *Remote Sensing of Environment*, **146**, 87–96.
16. Suggett, D., Kraay, G., Holligan, P., Davey, M., Jim, A. J. & Geider, R. (2001). Assessment of photosynthesis in a spring cyanobacterial bloom by use of a fast repetition rate fluorometer, *Limnology and Oceanography*, **46**(4), 802–810.
17. Platt, T., Gallegos, C. L. & Harrison, W. G. (1980). Photoinhibition of photosynthesis in natural assemblages of marine phytoplankton, *Journal of marine research*, **38**, 687–701.
18. Johnson, Z. (2000). Regulation of marine photosynthetic efficiency by photosystem II. PhD dissertation: botany, p. 189.
19. Teira, E., Mouriño, B., Marañón, E., Pérez, V., María, J. P., Serret P., Demetrio de Armas, Escánez, J., Woodward, E. M. S. & Fernández, E. (2005). Variability of chlorophyll and primary production in the Eastern North Atlantic Subtropical Gyre: potential factors affecting phytoplankton activity, *Deep-Sea Research I*, **52**, 569–588.
20. Tilstone, G., Smyth, T., Poulton, A. & Hutson, R. (2009). Measured and remotely sensed estimates of primary production in the Atlantic Ocean from 1998 to 2005, *Deep-Sea Research II*, **56**, 918–930.
21. Figueiras, F.G., Espinoza-González, O., Arbones, B., Garrido, J.L., Teixeira I.G. & Castro, C.G. (2014). Estimating phytoplankton size-fractionated primary production in the northwestern Iberian upwelling: Is mixotrophy relevant in pigmented nanoplankton? *Progress in Oceanography*, **128**, 88-97.
22. Longhurst A. (1995). Seasonal cycles of pelagic production and consumption, *Progress in Oceanography*, **36**, 77-167.
23. Lee, Z, Lance, V.P., Shang, S., Vaillancourt, R., Freeman, S., Lubac, B., Hargreaves, B. R., Carlos Del Castillo, Miller, R., Twardowski, M. & Wei, G. (2011). An assessment of optical properties and primary production derived from remote sensing in the Southern Ocean (SO GasEx), Journal of Geophysical Reseaech, **116**, C00F03, doi:10.1029/2010JC006747

24. Kahru, M., Jacox, M.G., Lee, Z., Kudela, R.M., Manzano-Sarabia, M. & Mitchell, B.G. (2015). Optimized multi-satellite merger of primary production estimates in the California Current using inherent optical properties, *Journal of Marine Systems*, **147**, 94-102.
25. Dogliotti, A.I., Lutz, V.A. & Segura, V. (2014). Estimation of primary production in the southern Argentine continental shelf and shelf-break regions using field and remote sensing data, *Remote Sensing of Environment*, **140**, 497–508.